Journal of Magnetic Resonance 206 (2010) 74–80

Contents lists available at ScienceDirect

Journal of Magnetic Resonance

journal homepage: www.elsevier.com/locate/jmr

In vivo ^{1}H NMR spectroscopy of the human brain at 9.4 T: Initial results

Dinesh Kumar Deelchand *, Pierre-François Van de Moortele, Gregor Adriany, Isabelle Iltis, Peter Andersen, John P. Strupp, J. Thomas Vaughan, Kâmil Uğurbil, Pierre-Gilles Henry

Center for Magnetic Resonance Research, Department of Radiology, University of Minnesota Medical School, Minneapolis, MN 55455, USA

ARTICLE INFO

Article history:
Received 20 November 2009
Revised 4 June 2010
Available online 10 June 2010

Keywords:
Proton NMR spectroscopy
Brain
Human
Relaxation times
Ultra-high field

ABSTRACT

In vivo proton NMR spectroscopy allows non-invasive detection and quantification of a wide range of biochemical compounds in the brain. Higher field strength is generally considered advantageous for spectroscopy due to increased signal-to-noise and increased spectral dispersion. So far ^{1}H NMR spectra have been reported in the human brain up to 7 T. In this study we show that excellent quality short echo time STEAM and LASER ^{1}H NMR spectra can be measured in the human brain at 9.4 T. The information content of the human brain spectra appears very similar to that measured in the past decade in rodent brains at the same field strength, in spite of broader linewidth in human brain. Compared to lower fields, the T_1 relaxation times of metabolites were slightly longer while T_2 relaxation values of metabolites were shorter (<100 ms) at 9.4 T. The linewidth of the total creatine (tCr) resonance at 3.03 ppm increased linearly with magnetic field (1.35 Hz/T from 1.5 T to 9.4 T), with a minimum achievable tCr linewidth of around 12.5 Hz at 9.4 T. At very high field, B_0 microsusceptibility effects are the main contributor to the minimum achievable linewidth.

1. Introduction

Higher signal-to-noise ratio (SNR) and spectral resolution at high magnetic fields have enabled significant gains in the quantification precision for a wide range of metabolites that can be measured using *in vivo* ^{1}H magnetic resonance spectroscopy (MRS). In rodents at 9.4 T, close to 20 metabolites can be reliably quantified in specific regions of the brain (“neurochemical profiles”) [1]. ^{1}H NMR spectra were also recently reported in rat brain at even higher fields, 14.1 T [2] and 16.4 T [3]. Numerous studies performed in the past decade have shown how such ^{1}H MRS measurements provide unique insights into brain biochemistry in normal brain and in animal models of brain disorders [4].

In the human brain, several studies reported gains in quantification precision at 3 T or 4 T compared to 1.5 T [5,6] and at 7 T compared to 3 T [7]. A more recent study found close to a 4-fold improvement in quantification precision at 7 T compared to 4 T [8]. At 7 T, up to 15 metabolites can be quantified reliably [9]. Gains in sensitivity have also been reported for ^{1}H spectroscopic imaging at 7 T compared to 1.5 T [10].

Such gains at high magnetic field have been achieved in spite of several limiting factors encountered at high fields. These include: longer T_1 and shorter T_2 relaxation times of metabolites, higher RF power deposition (SAR), lower available transmit B_1 RF field, stronger B_0 and B_1 inhomogeneity and increased spectral linewidth. In addition, the exact gain in quantification precision at high field is dependent on the experimental conditions (such as preamplifiers, RF coils and pulse sequences) and therefore difficult to determine precisely. Nonetheless, the fact that the quantification precision increases 4-fold from 4 T to 7 T [8] clearly shows the benefits of high fields for ^{1}H MRS up to 7 T in humans and suggests that further gains may be possible beyond 7 T.

Magnetic fields of 9.4 T recently became available for human studies and initial results of ^{1}H and ^{23}Na MRI of the human brain have been reported at such ultra-high field [11,12]. However, to the best of our knowledge, no *in vivo* ^{1}H NMR spectroscopy has been reported in human brain above 7 T.

In the present study we report the first ^{1}H NMR spectra acquired in the human brain at 9.4 T, obtained with two single-voxel methods, STEAM (TE = 8 ms) and LASER (TE = 41 ms), in the occipital lobe. T_1 and T_2 relaxation times of brain metabolites are also reported. The B_0 field dependence of the spectral linewidth and of the relaxation times of metabolites is also examined.

2. Materials and methods

2.1. Subjects and MR system

Six healthy subjects (20–55 years of age) participated in this study. Informed consent was obtained according to procedures ap-

* Corresponding author. Address: Center for Magnetic Resonance Research, University of Minnesota, 2021 6th St. SE, Minneapolis, MN 55455, USA. Fax: +1 612 626 2004.
E-mail address: dinesh@cmrr.umn.edu (D.K. Deelchand).

1090-7807/$ - see front matter © 2010 Elsevier Inc. All rights reserved.
doi:10.1016/j.jmr.2010.06.006

proved by the Institutional Review Board of the University of Minnesota. All experiments were performed using a 9.4 T/65 cm [11] horizontal bore magnet (Magnex Scientific Ltd, Oxford, UK) interfaced to a Varian DirectDrive console (Varian, Palo Alto, CA, USA) with eight independent transmit channels. The magnet system was equipped with an asymmetric self-shielded head gradient (40 cm inner diameter, maximum strength of 28.5 mT/m[1] with a rise time of 150 μs) powered by a Siemens gradient amplifier (Siemens AG, Medical Engineering, Erlangen, Germany). The subjects lay in a supine position with their head placed above an RF coil (described below) and wore earplugs throughout the study to attenuate the gradient acoustic noise.

A home-built half-volume RF probe covering the posterior half of the head and composed of eight ^{1}H microstrip elements (13 cm in length with a 12 mm wide copper strip conductor and a 4.2 cm wide RF ground plane, separated by a Teflon dielectric layer with a thickness of 12 mm) was used for both RF transmission and reception [13,14]. These elements were powered by one 1 kW and seven 500 W RF amplifiers (CPC, NY, USA). The 1 kW amplifier was connected to the coil element which was contributing the maximum transmit B_1 (B_1^+) in the region-of-interest based on the relative B_1 maps of the individual coil element. The applied RF power delivered to each coil element was continuously monitored with a 10 s and a 10 min moving average using an in-house built monitoring system. The latter consisted of directional couplers attached to each RF amplifiers. The power envelope of the RF waveform was continuously sampled by a calibrated ADC board. If the power of any coil were to exceed a predefined threshold, calculated based on FDA guidelines, then all RF amplifiers would be immediately shut down. To ensure safety, the threshold for the monitoring system was conservatively defined assuming that electric fields from all RF coils were to add constructively in the sample. Electromagnetic simulations were also performed to evaluate SAR. For this purpose, complex B_1 and E fields were generated for the eight-element microstrip RF coil loaded with a human head model using XFDTD software (Remcom Inc., PA, USA). SAR values were computed through the whole brain, taking into account the relative RF input power, B_1 shimming, RF pulse shapes, RF pulse durations and repetition time used for *in vivo* experiments. The resulting local and global SAR levels were found to be well below the FDA limits (data not shown).

2.2. NMR spectroscopy measurements

In order to minimize destructive B_1^+ interferences [15] in the single voxel used for spectroscopy (in this case located in the visual cortex), the relative phase of the transmit B_1^+ field for each coil element was optimized using a fast local B_1^+ shimming technique as recently described [16,17]. A series of low flip angle gradient-echo images were acquired while transmitting RF power through one coil element at a time and receiving with all eight elements simultaneously. The relative transmit phase for each coil element was optimized in order to obtain maximal B_1 in the region-of-interest using Matlab (The MathWorks Inc., Natick, MA, USA). Signals from all eight channels were acquired using a digital receiver system that was developed in-house; this receiver used an Echotek (Huntsville, AL, USA) ECDR-814 board to oversample the 20-MHz intermediate frequency (IF) at 64 MHz and 14-bit resolution, with digital band-pass filtering.

Using transverse and sagittal gradient-echo images obtained after B_1^+ shimming, a volume-of-interest (VOI) of 8 ml ($2 \times 2 \times 2$ cm^3) was positioned in the visual cortex. All first- and second-order shim terms were automatically adjusted using a multi-transmit version of FAST(EST)MAP [18] resulting in a water linewidth of 15.7 ± 1.4 Hz (full width at half height). The water linewidth did not improve when the voxel size was decreased from 8 ml to 1 ml indicating that macroscopic B_0 shimming was optimal.

Single-voxel localization was achieved using STEAM with TE of 8 ms (1.5 ms asymmetric RF pulses, 4.5 kHz bandwidth) transmitting on all eight elements with the same RF power and the phases determined from the B_1 shimming procedure. Water suppression was performed with VAPOR using eight RF pulses with variable pulse power and optimized timing [19]. To suppress unwanted signal outside the volume-of-interest, outer volume suppression (OVS) pulses were also applied as described in [19]. The OVS scheme was made up of four blocks, each consisting of at least six slice-selective hyperbolic-secant RF pulses (6 ms duration, 7 kHz bandwidth) followed by gradient spoilers. These OVS modules were interleaved with the water suppression pulses. Spectra were acquired with a repetition time of 6 s, 8 k complex data points and spectral width of 8 kHz. Each free induction decay (FID) was individually saved for subsequent scan-to-scan frequency correction. A water reference spectrum was also recorded in order to perform eddy current correction and to serve as a concentration reference for absolute quantification. Macromolecule spectra were acquired using the inversion-recovery technique with the inversion time optimized to null the signals from metabolites.

^{1}H NMR spectra were also acquired using LASER (Localization by Adiabatic SElective Refocusing, [20]) with TE = 41 ms. The sequence consisted of a 3 ms nonselective adiabatic half-passage pulse followed by three pairs of slice-selective adiabatic full-passage pulses (2.5 ms duration, 4.8 kHz bandwidth, HS4 modulation) for 3D-localization. Water suppression was also achieved with VAPOR. Spectra were acquired with a repetition time of 6 s with 8 k of data points and spectral width of 8 kHz.

In both pulse sequences, the transmitter frequency was set at 2.65 ppm (close to the NAA multiplets). This resulted in a ~13% displacement artifact for resonances at the edges of the detected spectrum (4.2 ppm and 1.1 ppm) compared to the nominal voxel selection.

2.3. Measurements of relaxation times

T_1 relaxation times of metabolites were measured using STEAM preceded by an adiabatic inversion pulse. An echo time of 80 ms was chosen in order to minimize signals from macromolecules, which have a much shorter T_2 than metabolites. Six different inversion times t_{IR} were used (0.006, 0.22, 0.45, 1.75, 3 and 5 s). Spectra were acquired under nearly fully relaxed conditions with a delay of 6 s between acquisition of each fid and the next inversion pulse and with 32 repetitions. Metabolite T_1 values were obtained by fitting the relative concentrations obtained after LCModel analysis of the inversion-recovery ^{1}H spectra using a single exponential function with 3 fitted parameters. T_1 values for *J*-coupled metabolites were not estimated due to the relatively long TE used in these measurements.

For T_2 relaxation times measurements, spectra were collected at seven different echo times: 70, 80, 90, 100, 120, 150 and 200 ms with a repetition time of 6 s. For each echo time, 32 averages were acquired except for TE $\geqslant$ 150 ms where 64 averages were recorded in order to increase the signal-to-noise ratio. Signals from macromolecule resonances were negligible at these long TEs. Metabolite T_2 relaxation times were determined by fitting the relative concentrations obtained after LCModel analysis of ^{1}H spectra using a single exponential delay function with 2 fitted parameters.

[1] The gradient amplifier was not optimal which limited the maximum gradient strength compared to the maximum theoretically available for this gradient coil (50 mT/m).

2.4. Processing and quantitation of in vivo spectra

All spectral pre-processing was performed in Matlab. Water suppressed FIDs acquired from each coil element were corrected for eddy current by using their corresponding water reference scan. After eddy current correction, all FIDs had similar phase. These FIDs were individually corrected for any B_0 frequency shift then summed together after applying a weighting factor for each channel in order to maximize the SNR of the summed spectrum. The weighting factor was based on the SNR of each individual channel determined from their N-acetyl aspartate (NAA) peak [21,22].

All ^{1}H NMR spectra were analyzed using LCModel (Stephen Provencher Inc., Oakville, ON, Canada). The basis spectra for each detectable brain metabolite were simulated using home-written programs based on density matrix formalism in Matlab with measured and published chemical shifts and *J*-coupling values [23]. No baseline correction, zero-filling or apodization functions were applied to the *in vivo* weighted summed data prior to the analysis.

3. Results and discussion

3.1. Local B_1^+ phase shimming

At high magnetic field, destructive interferences can severely reduce the available B_1^+. High peak B_1^+ is highly desirable for NMR spectroscopy in order to minimize the duration of the RF pulses, thereby reducing the echo time and chemical-shift displacement artifacts. Maximizing B_1^+ efficiency is also critical to minimize SAR, particularly at high field where SAR deposition is more likely to become a limiting factor.

One way to maximize the available B_1^+ over a region-of-interest at high field is to perform local B_1^+ shimming [16,17]. Fig. 1 demonstrates the gain in transmit B_1 obtained using B_1^+ shimming with our setup at 9.4 T. The maximum B_1^+ was 205 Hz across the defined region-of-interest in the occipital lobe after B_1 phase shimming versus only 60 Hz before B_1^+ shimming, corresponding to a 10 dB gain in transmit power efficiency. Note that these B_1^+ maps were acquired with an RF power well below the maximum power available in order to remain within SAR limits. Based on the measured B_1^+ maps at low power, we extrapolated that the maximum B_1^+ available for this particular experimental setup was ~1.5 kHz in the occipital lobe when using the full transmit power available with our RF amplifiers (1 kW RF amplifier output on the channel with the highest B_1^+ contribution in the VOI and 500 W amplifier output on the remaining seven channels). This maximal B_1^+ value was also confirmed directly from the calibration of RF pulses in STEAM at full power. Note that only about half of the transmitted power was actually available at the coil ports due to losses in the cables.

In the particular case shown in Fig. 1, the relative transmit phase of each element (from 1 to 8) after B_1^+ shimming was: 0, 33, 20, 319, 284, 292, 297 and 322° where element #1 was arbitrarily chosen as the reference phase with 0°. This optimal phase for each element after B_1^+ phase shimming was generally reproducible from one subject to the next, with the biggest subject-to-subject variations (up to 40°) for element #7. STEAM ^{1}H spectra acquired with each of the eight individual coil elements are also shown in Fig. 1. The highest receive sensitivity for the VOI illustrated in Fig. 1 was obtained with elements #4–7. Summing spectra from all eight elements (after weighting each spectrum with their SNR [21,22]) further increased the SNR by ~20% compared to the case when only the four spectra with the highest SNR (elements #4–7) were used.

3.2. In vivo proton NMR spectra

We assessed the feasibility of ^{1}H NMR spectroscopy with two single-voxel sequences widely used in our and other laboratories, namely STEAM and LASER.

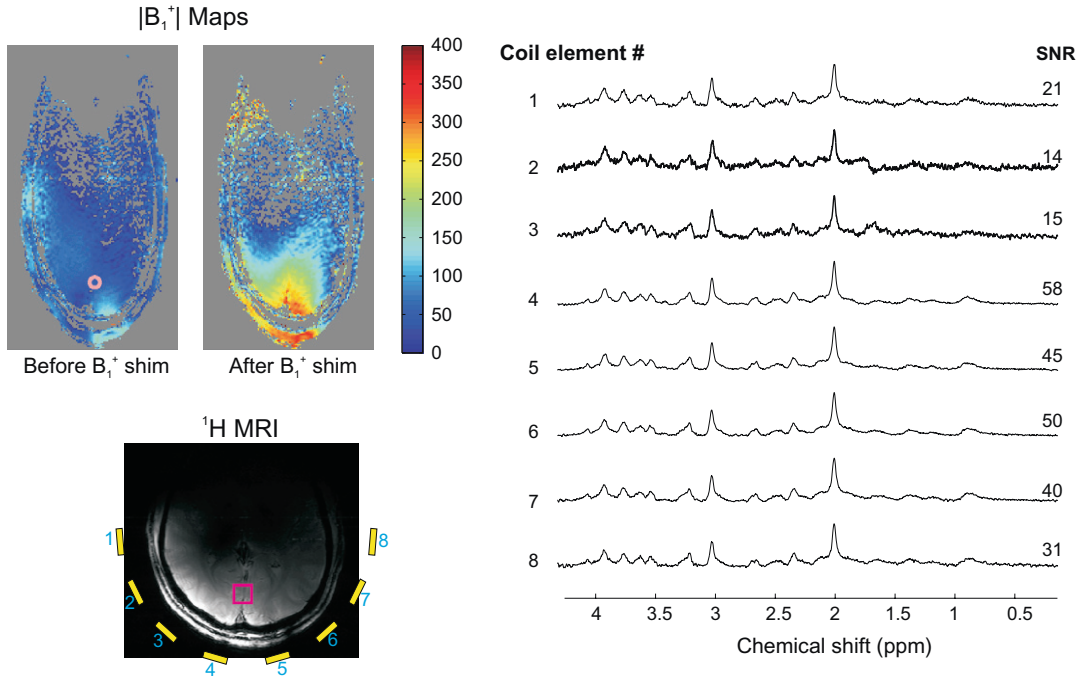

Fig. 1. *Top left.* The two color pictures show the absolute B_1^+ maps in Hz before and after local B_1^+ phase shimming, optimized for the region-of-interest shown as a pink circle in the occipital lobe on the left picture ($|B_1^+|$ maps were obtained using AFI [50] with: TR1/TR2/TE = 25/125/5 ms, FOV = 20 × 20 × 12 mm, data matrix = 256 × 64 × 24). Note the very substantial increase in $|B_1^+|$ after B_1 shimming. *Bottom left.* Gradient-echo axial image after B_1^+ shimming. The eight yellow bars (labeled 1–8) indicate the position of the eight coil elements. *Right.* ^{1}H NMR spectra from each coil element (labeled 1–8 on the left vertical axis), acquired in an 8 ml VOI (denoted by the red square on the bottom left image) with STEAM (TE = 8 ms, NT = 32). The respective SNR is shown on the right end of each spectrum. Note that the spectra were sampled with the eight coil elements simultaneously. Each spectrum was scaled to have the same NAA peak intensity.

3.3. STEAM spectra

^{1}H NMR STEAM spectra obtained in the human brain at 9.4 T at very short echo time (TE = 8 ms, NT = 384) showed excellent spectral quality (Fig. 2, top). There was no noticeable baseline distortion or contamination by signals from outside the voxel (such as lipids), indicating satisfactory outer volume suppression (OVS). Excellent water suppression was also consistently achieved, as illustrated by the small water residual observed in all subjects. The spectrum was dominated by strong singlet resonances of NAA, Cho, Cr and PCr as expected. The glutamate multiplet at 2.35 ppm was clearly resolved from neighboring resonances such as glutamine (2.45 ppm). Contributions from smaller resonances such as aspartate and GABA were also noticeable.

The human brain STEAM proton spectrum had an overall spectral pattern very similar to that obtained in the rat brain at the same field strength (Fig. 2, bottom). However the spectral linewidth was noticeably smaller in rat brain (8–10 Hz, [1]) compared to human brain (~13 Hz) due to longer T_2 and smaller microsusceptibility effects. In addition, several metabolites showed different intensities in human brain compared to rat brain. For instance, taurine (3.2–3.4 ppm) and lactate (1.3 ppm) levels were lower in human than in the rat brain. Note that the concentration of taurine is known to be different across species [24] and that the higher lactate concentration observed in the rat is explained by the use of isoflurane anesthesia in this particular animal.

3.4. LASER spectra

In addition to STEAM spectra, LASER ^{1}H NMR spectra were also acquired at a minimum TE of 41 ms (NT = 168, Fig. 3). Even at this relatively longer TE, signals from strongly coupled resonances such as glutamate or the multiplet of NAA were still being observed as expected, since the Carr-Purcell pulse train employed in LASER [20] minimizes *J*-evolution. Macromolecule resonances were strongly reduced compared to the STEAM spectrum (Fig. 2) due to their short T_2 relaxation times.

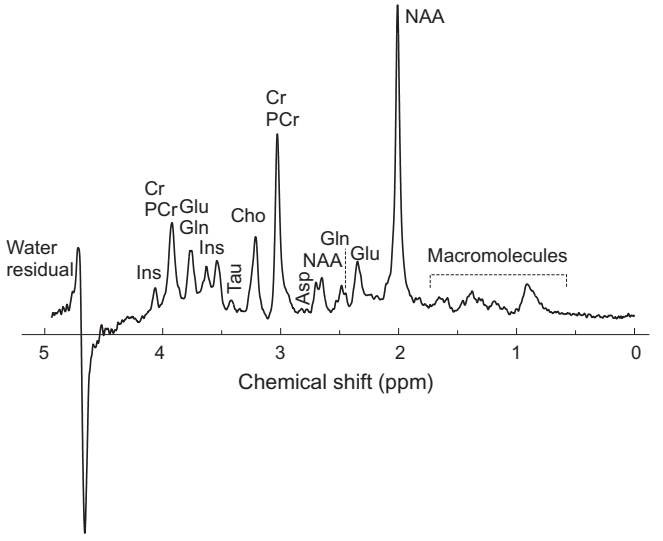

Fig. 3. Weighted summed *in vivo* ^{1}H LASER spectrum (TE = 41 ms, VOI = 6 ml, 168 scans, gf = 0.09, lb = −2) acquired from the human visual cortex at 9.4 T.

3.5. Absolute quantification of short echo time STEAM spectrum

LCModel analysis of *in vivo* ^{1}H STEAM spectrum (TE = 8 ms, TM = 35 ms, 32 averages, occipital lobe) has allowed the absolute concentration of at least 15 metabolites to be reliably determined (Table 1) using the water peak of the unsuppressed reference scan as an internal concentration reference. These concentrations were in excellent agreement with previously published data [6,9]. Cramer-Rao Lower Bounds (CRLBs) were also below 20% (Table 1) for most metabolites, except those at a very low concentration (< 0.5 μmol/g).

The CRLBs of metabolites obtained in this study were comparable to those obtained at 7 T using STEAM [9] and slightly lower than those reported in another 7 T study with SPECIAL pulse se-

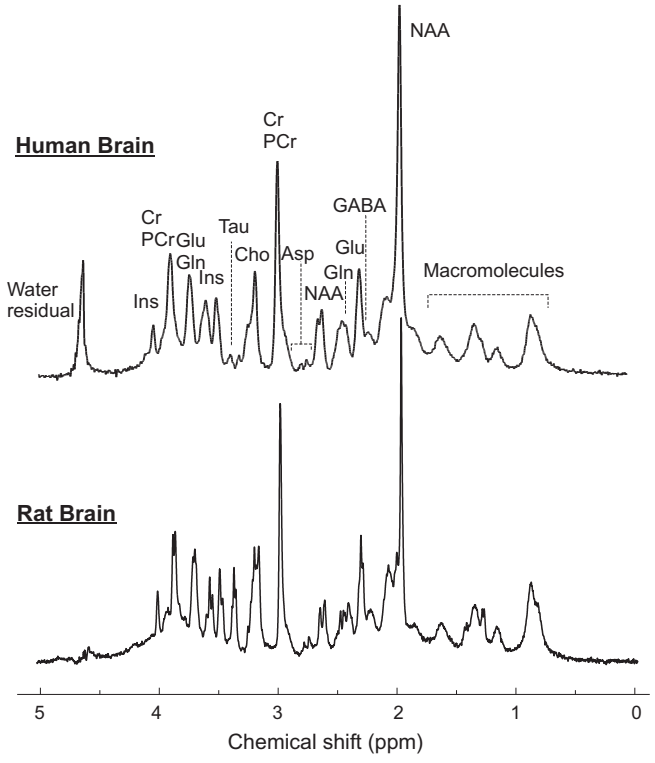

Fig. 2. Comparison between a STEAM ^{1}H NMR spectrum acquired *in vivo* at 9.4 T from the human visual cortex (top, VOI = 8 ml, TE = 8 ms, TM = 35 ms, lb (line broadening) = −3, gf (Gaussian factor) = 0.15, 384 scans) and a similar spectrum acquired in rat brain (bottom, VOI = 65 μl, TE = 2 ms, lb = −1, gf = 0.25, 640 scans, courtesy of Dr. I. Tkáč). Human data represents the weighted sum from all eight coil elements using the spectral processing steps described in the Methods section.

Table 1
Concentrations of cerebral metabolites in the human brain measured at 9.4 T after LCModel analysis of six STEAM spectra (TE = 8 ms, 32 averages each) from six subjects. Data represent mean ± standard deviation.

Metabolites	Concentration (μmol/g)	CRLB (%)
Creatine	3.2 ± 0. 5	7.4 ± 1.7
Phosphocreatine	4.5 ± 0.4	5.3 ± 1.0
Creatine + Phosphocreatine	7.7 ± 0.4	2.0 ± 0.0
Total Choline (GPC + PCho)	0.9 ± 0.2	5.7 ± 1.4
NAA	13.5 ± 1.6	1.9 ± 0.4
Glutamate	9.3 ± 0.9	2.0 ± 0.0
Glutamine	2.2 ± 0.2	6.9 ± 0.9
Myo-inositol	5.3 ± 0.4	3.0 ± 0.6
Glutathione	1.1 ± 0.3	8.9 ± 3.4
GABA	1.3 ± 0.4	12.4 ± 3.6
NAAG	1.1 ± 0.5	18.7 ± 7.5
Taurine	1.3 ± 0.2	11.4 ± 2.3
Phosphethanolamine	1.6 ± 0.4	10.7 ± 2.3
Aspartate	2.1 ± 0.5	14.4 ± 5.2
Lactate	0.5 ± 0.1	23.4 ± 10.5
Alanine	0.3 ± 0.3	35.4 ± 29.0
Scyllo-inositol	0.3 ± 0.2	39.7 ± 42.8

quence [7]. We would like to emphasize that comparing sensitivity at 9.4 T with that at lower fields was not our objective in this initial study. Such comparisons require careful matching of RF coil designs and acquisitions conditions on different MR systems. The eight-element microstrip RF coil used in this study may not provide optimal sensitivity for spectroscopy in the occipital lobe. We expect that further developments in RF coil design will lead to improvements in sensitivity.

3.6. T_1 and T_2 relaxation times of brain metabolites

Measured T_1 and apparent T_2 relaxation times for the singlet resonances of NAA, total creatine and total choline are reported in Table 2.

The T_1 relaxation times of metabolites were measured using STEAM preceded by inversion-recovery. The longest T_1 values were found for the methyl groups of NAA and total creatine. The T_1 relaxation time for the CH_2 resonance of total creatine was significantly shorter than that for the CH_3 resonance as expected from previous studies.

T_2 relaxation times were measured using STEAM at multiple echo times. All apparent T_2 relaxation times were below 100 ms (Table 2). The CH_3 resonance of NAA had the longest apparent T_2 (98 ms) and the CH_2 and CH_3 resonances of total creatine had almost identical apparent T_2 values; 68.3 ms and 71.9 ms respectively.

3.7. B_0 field dependence of relaxation times

T_1 and T_2 relaxation times of metabolites measured at 9.4 T were compared to values from literatures at lower fields (T_1: [25–34]; T_2: [9,25–43]; Fig. 4). Only values from studies using STEAM or PRESS were retained for this comparison.

T_1 relaxation times of metabolites in human brain at 9.4 T were slightly longer than at lower fields, i.e. 1.5, 4 and 7 T (Fig. 4, left) although no clear B_0 field dependence could be established due to the relatively large dispersion in the reported T_1 values at lower fields.

In contrast, T_2 relaxations of metabolites were significantly shorter in humans at 9.4 T (Fig. 4, right) than at lower fields. On average, the apparent T_2 relaxation times in human at 9.4 T were ~30% shorter than at 7 T [9]. This is consistent with the decrease in T_2 relaxation times with B_0 demonstrated in a number of previous studies in both humans and animals [25,40,42,43].

Based on the T_2 values at various field strengths (from 1.5 to 9.4 T, Fig. 4), relaxation rates R_2 (i.e. $1/T_2$) as a function of B_0 were fitted with a quadratic function in the form ($A\,B_0^n + C$). The term C can be attributed to dipole–dipole relaxation ($R_{2,dd}$) which is virtually independent of B_0 and was found to have values of several seconds^{-1} ($C = 2.6 \pm 0.6\ s^{-1}$ and $C = 3.8 \pm 0.7\ s^{-1}$ for methyl group of NAA and tCr respectively) consistent with previous studies [44]. The fitted parameter n corresponding to the best fit was $n = 1.7 \pm 0.4\ s^{-1}$ and $n = 1.3 \pm 0.2\ s^{-1}$ for the CH_3 group of NAA and tCr respectively. The B_0-dependent term (proportional to B_0^n) can be attributed to a large extent to increased dynamic dephasing due to increased local susceptibility gradients as recently suggested by Michaeli et al. [40,44]. These susceptibility fields result in a loss of phase coherence between spins thereby shortening the T_2. The effect of this signal loss can be minimized considerably by placing a Carr-Purcell pulse train between excitation and signal acquisition. Examples of such pulse sequence are CP-PRESS [35] and CP-LASER [40] where the apparent T_2 times of metabolites is prolonged. The observation that $n < 2$ (statistically significant only for tCr and not for NAA) must be taken with caution, as the fitted data come from multiple studies published by different groups with different techniques and potentially variable diffusion weighting with increasing TE.

3.8. Comparison of relaxation times in human and rat brain

T_1 relaxation times of metabolites were generally longer in human compared to rat brain at 9.4 T (Table 3). For example, T_1 for the methyl group of NAA was 1.78 s in human versus 1.41 s in rat brain at 9.4 T [1].

In contrast, the apparent T_2 relaxation values were shorter in human compared to rat brain at the same field strength (Table 3). For example, the mean apparent T_2 of methyl group of NAA was 98 ms in human versus 190 ± 15 ms in rat brain at 9.4 T [1,45,46].

Differences in T_1 and T_2 relaxation times between human and rat brain at 9.4 T may be explained in part by differences in the structural organization of the brain. For example, in the rat brain

Table 2
T_1 and apparent T_2 relaxation times (mean ± SD) of metabolites measured in the brain of six healthy subjects at 9.4 T using STEAM sequence. T_1 values were fitted with $R^2 \geqslant 0.96$ and T_2 with $R^2 \geqslant 0.97$.

Metabolites	T_1 (ms)	T_2 (ms)
NAA singlet	1777 ± 82	98.0 ± 8.4
Total Creatine (CH_3 group)	1746 ± 133	71.9 ± 5.0
Total Creatine (CH_2 group)	1030 ± 270	68.3 ± 6.4
Total Choline	1513 ± 153	70.7 ± 7.1

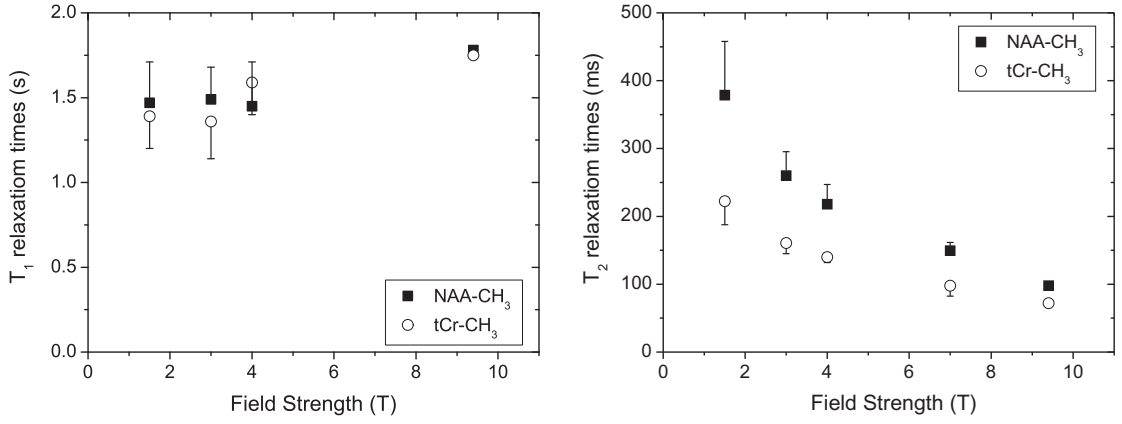

Fig. 4. T_1 and T_2 relaxation times as a function of static B_0 field strength for the methyl resonance of NAA and total creatine measured in the human brain using STEAM and/or PRESS. Data points with error bars represent the mean and standard deviation of published relaxation times at each field strength.

Table 3
Comparison of T_1 and T_2 relaxation times of methyl group of NAA and tCr between human and animal (rat) brain at 9.4 T.

Metabolites	T_1 (s)		T_2 (ms)	
	Human (current study)	Animal [1]	Human (current study)	Animal [1,45,46]
NAA	1.78	1.41	98	190
tCr	1.75	1.34	72	117.7

local susceptibility gradients are likely smaller than in humans, and therefore spin dephasing would be less pronounced than in human brain which would cause longer T_2.

3.9. Comparison of linewidths at different B_0 values

In the present study, the minimum *in vivo* linewidth measured on the methyl resonance of total creatine was ~12.5 Hz after FASTEST(EST)MAP was used to adjust all first- and second-order shim terms. Reducing the voxel size did not yield a narrower linewidth, indicating that B_0 macroscopic shimming was optimal. This minimum achievable linewidth was markedly larger than at lower fields [9] (Fig. 5) with a linear relationship between the minimum achievable linewidth and B_0, corresponding to a linewidth increase of 1.35 ± 0.02 Hz/T. The linewidth measured in humans at 9.4 T was also broader compared to that reported in adult rat brain (~9 Hz [1]) at 9.4 T, consistent with the shorter T_2 values observed in human brain.

Line broadening due to microscopic susceptibility effect (Δv^*), T_2 relaxation effects ($(\pi T_2)^{-1}$) and chemical shift difference ($\Delta\delta$) were calculated based on the *in vivo* measured linewidth of the CH_3 group of total creatine for three different fields strengths (Fig. 5) using the following equation: $\Delta v^* = (\Delta v_{1/2} - (\pi T_2)^{-1} - \Delta\delta)$. This result clearly shows that microscopic susceptibility effects are the main factor contributing to the line broadening as the field strength increases since the contribution of the relaxation pathways via dipolar mechanisms to T_2 are relatively small compared to the relaxations induced by local magnetic susceptibilities [44].

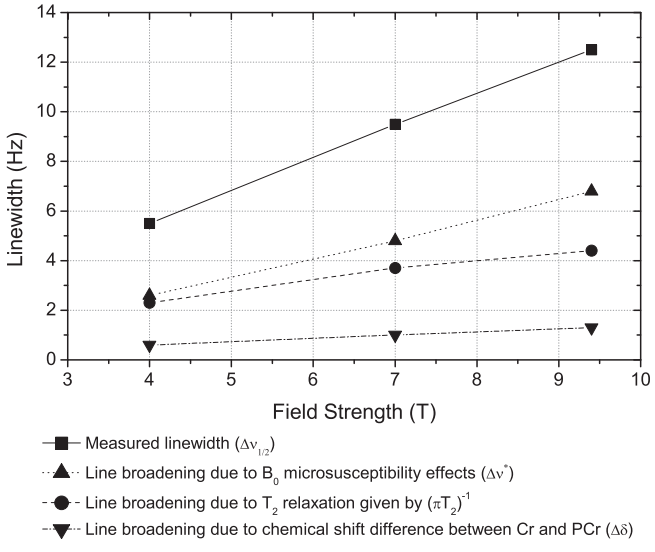

Fig. 5. Microscopic susceptibility effect (Δv^*) as a function of field strengths based on the experimentally determined linewidth ($\Delta v_{1/2}$) of the methyl group of total creatine in human brain. Δv^* is defined as $(\Delta v_{1/2} - (\pi T_2)^{-1} - \Delta\delta)$ where T_2 is the transverse relaxation of the CH_3 group of total creatine. The chemical shift difference between Cr and PCr resonances ($\Delta\delta$) was set to 0.0033 ppm as determined on high-resolution phantom data. Data points at 4 and 7 T were taken from [9].

3.10. Future perspectives

The main objective of this paper was to show the feasibility of acquiring high quality ^{1}H MRS in the human brain at 9.4 T and to provide reference data for the minimum linewidth and for relaxations times in human brain at 9.4 T. Further work is needed to assess potential sensitivity gains at 9.4 T compared to 7 T. The sensitivity of the eight-channel microstrip RF coil used in the present study may not be optimal for MRS in the occipital lobe. Comparing sensitivity at 9.4 T and 7 T will require careful matching of RF coils and other acquisition conditions on different systems, similar to what was done recently when comparing 7 T with 4 T [8]. Given the significant gains at 7 T compared to 4 T, one can reasonably expects sensitivity gains at 9.4 T compared to 7 T. This, however, remains to be demonstrated, and the potential gains may vary depending on brain location. Sensitivity gains would allow measurement in deep brain structures, such as hippocampus, and smaller volumes.

Other spectroscopic measurements may also benefit from 9.4 T in spite of the added challenges. For example, spectral editing would benefit from ultra-high field since signals separation arising from larger chemical shift dispersion increases with field strength [47], although some of the gain in selectivity would be offset by signal loss due to shorter T_2 relaxation times. Improved sensitivity in spectroscopic imaging (i.e. smaller voxel with the ability to distinguish different tissues types) is also expected, especially in the view of recent result reported at 7 T [48].

4. Conclusions

In this study, we demonstrated high quality ^{1}H NMR spectra measured *in vivo* in the human brain at 9.4 T and these spectra were very similar to that obtained in the past decade in rodent brains at the same field strength [1,19,45,49]. We also observed that T_2 relaxation times of metabolites were shorter at 9.4 T than at 7 T, although signal loss due to T_2 relaxation was still largely negligible at an echo time of 8 ms. The minimum achievable linewidth increased with B_0 field strength (1.35 Hz/T from 1.5 T to 9.4 T) and our results indicate that, at very high field of 9.4 T, B_0 microsusceptibility effects are the main contributor to the minimum linewidth that can be achieved *in vivo*.

Acknowledgments

The authors thank Drs. Ivan Tkáč, Lance DelaBarre, Uzay Emir, Michael Garwood and Shalom Michaeli for helpful discussions and Dr. Xiaoping Wu for SAR simulations. This work was supported by NIH Grants: P41RR008079, P30NS057091, R01NS038672, R01EB006835 and the Keck Foundation.

References

[1] J. Pfeuffer, I. Tkac, S.W. Provencher, R. Gruetter, Toward an in vivo neurochemical profile: quantification of 18 metabolites in short-echo-time (1)H NMR spectra of the rat brain, J. Magn. Reson. 141 (1999) 104–120.
[2] V. Mlynarik, C. Cudalbu, L. Xin, R. Gruetter, 1H NMR spectroscopy of rat brain in vivo at 14.1 Tesla: improvements in quantification of the neurochemical profile, J. Magn. Reson. 194 (2008) 163–168.
[3] D.Z. Balla, S.-T. Hong, G. Shajan, R. Pohmann, K. Ugurbil, Single voxel MR spectroscopy with echo times below 2 ms at 16.4 T in the rat brain: first in vivo results, Proc. Int. Soc. Mag. Reson. Med. 16 (2008) 3295.
[4] I. Tkac, C.D. Keene, J. Pfeuffer, W.C. Low, R. Gruetter, Metabolic changes in quinolinic acid-lesioned rat striatum detected non-invasively by in vivo (1)H NMR spectroscopy, J. Neurosci. Res. 66 (2001) 891–898.
[5] O. Gonen, S. Gruber, B.S. Li, V. Mlynarik, E. Moser, Multivoxel 3D proton spectroscopy in the brain at 1.5 versus 3.0 T: signal-to-noise ratio and resolution comparison, AJNR Am. J. Neuroradiol. 22 (2001) 1727–1731.
[6] R. Bartha, D.J. Drost, R.S. Menon, P.C. Williamson, Comparison of the quantification precision of human short echo time (1)H spectroscopy at 1.5 and 4.0 Tesla, Magn. Reson. Med. 44 (2000) 185–192.

[7] R. Mekle, V. Mlynárik, G. Gambarota, M. Hergt, G. Krueger, R. Gruetter, MR spectroscopy of the human brain with enhanced signal intensity at ultrashort echo times on a clinical platform at 3 T and 7 T, Magn. Reson. Med. 61 (2009) 1279–1285.
[8] I. Tkac, G. Oz, G. Adriany, K. Ugurbil, R. Gruetter, In vivo 1H NMR spectroscopy of the human brain at high magnetic fields: metabolite quantification at 4 T vs. 7 T, Magn. Reson. Med. 62 (2009) 868–879.
[9] I. Tkac, P. Andersen, G. Adriany, H. Merkle, K. Ugurbil, R. Gruetter, In vivo 1H NMR spectroscopy of the human brain at 7 T, Magn. Reson. Med. 46 (2001) 451–456.
[10] R. Otazo, B. Mueller, K. Ugurbil, L. Wald, S. Posse, Signal-to-noise ratio and spectral linewidth improvements between 1.5 and 7 Tesla in proton echo-planar spectroscopic imaging, Magn. Reson. Med. 56 (2006) 1200–1210.
[11] T. Vaughan, L. DelaBarre, C. Snyder, J. Tian, C. Akgun, D. Shrivastava, W. Liu, C. Olson, G. Adriany, J. Strupp, P. Andersen, A. Gopinath, P.F. van de Moortele, M. Garwood, K. Ugurbil, 9.4 T human MRI: preliminary results, Magn. Reson. Med. 56 (2006) 1274–1282.
[12] I.C. Atkinson, L. Renteria, H. Burd, N.H. Pliskin, K.R. Thulborn, Safety of human MRI at static fields above the FDA 8 T guideline: sodium imaging at 9.4 T does not affect vital signs or cognitive ability, J. Magn. Reson. Imag. 26 (2007) 1222–1227.
[13] G. Adriany, D. Deelchand, P.G. Henry, J. Tian, J.T. Vaughan, K. Ugurbil, P.F. Van de Moortele, A 16 channel T/R Open-Faced Head Array for Humans at 9.4 T, Proc. Int. Soc. Mag. Reson. Med. 17 (2009) 3005.
[14] J.T. Vaughan, RF Coil for Imaging System, US Patent Serial No. 6, vol. 633, 2003, p. 161.
[15] P.F. Van de Moortele, C. Akgun, G. Adriany, S. Moeller, J. Ritter, C.M. Collins, M.B. Smith, J.T. Vaughan, K. Ugurbil, B(1) destructive interferences and spatial phase patterns at 7 T with a head transceiver array coil, Magn. Reson. Med. 54 (2005) 1503–1518.
[16] G.J. Metzger, C. Snyder, C. Akgun, T. Vaughan, K. Ugurbil, P.F. Van de Moortele, Local B1+ shimming for prostate imaging with transceiver arrays at 7 T based on subject-dependent transmit phase measurements, Magn. Reson. Med. 59 (2008) 396–409.
[17] P.-F. Van De Moortele, C. Snyder, L. DelaBarre, C. Akgun, X. Wu, J. Vaughan, and K. Ugurbil, Fast mapping of relative B1+ phase in the human head at 9.4 Tesla with a 14 channel transceive coil array. In: Int. Symposium on Biomedical Magnetic Resonance Imaging and Spectroscopy at Very High Fields, Wurzburg, Germany 2006.
[18] R. Gruetter, I. Tkac, Field mapping without reference scan using asymmetric echo-planar techniques, Magn. Reson. Med. 43 (2000) 319–323.
[19] I. Tkac, Z. Starcuk, I.Y. Choi, R. Gruetter, In vivo 1H NMR spectroscopy of rat brain at 1 ms echo time, Magn. Reson. Med. 41 (1999) 649–656.
[20] M. Garwood, L. DelaBarre, The return of the frequency sweep: designing adiabatic pulses for contemporary NMR, J. Magn. Reson. 153 (2001) 155–177.
[21] C.J. Hardy, P.A. Bottomley, K.W. Rohling, P.B. Roemer, An NMR phased array for human cardiac 31P spectroscopy, Magn. Reson. Med. 28 (1992) 54–64.
[22] S.M. Wright, L.L. Wald, Theory and application of array coils in MR spectroscopy, NMR Biomed. 10 (1997) 394–410.
[23] V. Govindaraju, K. Young, A.A. Maudsley, Proton NMR chemical shifts and coupling constants for brain metabolites, NMR Biomed. 13 (2000) 129–153.
[24] M. Puka, K. Sundell, J.W. Lazarewicz, A. Lehmann, Species differences in cerebral taurine concentrations correlate with brain water content, Brain Res. 548 (1991) 267–272.
[25] F. Traber, W. Block, R. Lamerichs, J. Gieseke, H.H. Schild, 1H metabolite relaxation times at 3.0 Tesla: measurements of T_1 and T_2 values in normal brain and determination of regional differences in transverse relaxation, J. Magn. Reson. Imag. 19 (2004) 537–545.
[26] R. Kreis, J. Slotboom, L. Hofmann, C. Boesch, Integrated data acquisition and processing to determine metabolite contents, relaxation times, and macromolecule baseline in single examinations of individual subjects, Magn. Reson. Med. 54 (2005) 761–768.
[27] D. Rutgers, J.. van der Grond, Relaxation times of choline, creatine and N-acetyl aspartate in human cerebral white matter at 1.5 T, NMR Biomed. 15 (2002) 215–221.
[28] J. Frahm, H. Bruhn, M.L. Gyngell, K.D. Merboldt, W. Hanicke, R. Sauter, Localized high-resolution proton NMR spectroscopy using stimulated echoes: initial applications to human brain in vivo, Magn. Reson. Med. 9 (1989) 79–93.
[29] T. Ethofer, I. Mader, U. Seeger, G. Helms, M. Erb, W. Grodd, A. Ludolph, U. Klose, Comparison of longitudinal metabolite relaxation times in different regions of the human brain at 1.5 and 3 Tesla, Magn. Reson. Med. 50 (2003) 1296–1301.
[30] C.G. Choi, J. Frahm, H. Bruhn, M.L. Gyngell, K.D. Merboldt, W. Hanicke, R. Sauter, Localized proton MRS of the human hippocampus: metabolite concentrations and relaxation times. Localized high-resolution proton NMR spectroscopy using stimulated echoes: initial applications to human brain in vivo, Magn. Reson. Med. 41 (1999) 204–207.
[31] V. Mlynarik, S. Gruber, E. Moser, Proton T (1) and T (2) relaxation times of human brain metabolites at 3 Tesla, NMR Biomed. 14 (2001) 325–331.
[32] R. Srinivasan, N. Sailasuta, R. Hurd, S. Nelson, D. Pelletier, Evidence of elevated glutamate in multiple sclerosis using magnetic resonance spectroscopy at 3 T, Brain 128 (2005) 1016–1025.
[33] S. Posse, C.A. Cuenod, R. Risinger, D. Le Bihan, R.S. Balaban, Anomalous transverse relaxation in 1H spectroscopy in human brain at 4 Tesla, Magn. Reson. Med. 33 (1995) 246–252.
[34] H.P. Hetherington, G.F. Mason, J.W. Pan, S.L. Ponder, J.T. Vaughan, D.B. Twieg, G.M. Pohost, Evaluation of cerebral gray and white matter metabolite differences by spectroscopic imaging at 4.1 T, Magn. Reson. Med. 32 (1994) 565–571.
[35] B.J. Soher, P.M. Pattany, G.B. Matson, A.A. Maudsley, Observation of coupled 1H metabolite resonances at long TE, Magn. Reson. Med. 53 (2005) 1283–1287.
[36] E.E. Brief, K.P. Whittall, D.K. Li, A.L. MacKay, Proton T_2 relaxation of cerebral metabolites of normal human brain over large TE range, NMR Biomed. 18 (2005) 14–18.
[37] P.B. Barker, D.O. Hearshen, M.D. Boska, Single-voxel proton MRS of the human brain at 1.5 T and 3.0 T, Magn. Reson. Med. 45 (2001) 765–769.
[38] C. Choi, N.J. Coupland, P.P. Bhardwaj, S. Kalra, C.A. Casault, K. Reid, P.S. Allen, T_2 measurement and quantification of glutamate in human brain in vivo, Magn. Reson. Med. 56 (2006) 971–977.
[39] F. Schubert, J. Gallinat, F. Seifert, H. Rinneberg, Glutamate concentrations in human brain using single voxel proton magnetic resonance spectroscopy at 3 Tesla, Neuroimage 21 (2004) 1762–1771.
[40] S. Michaeli, M. Garwood, X.H. Zhu, L. DelaBarre, P. Andersen, G. Adriany, H. Merkle, K. Ugurbil, W. Chen, Proton T_2 relaxation study of water, N-acetylaspartate, and creatine in human brain using Hahn and Carr-Purcell spin echoes at 4 T and 7 T, Magn. Reson. Med. 47 (2002) 629–633.
[41] R. Gruetter, M. Garwood, K. Ugurbil, E.R. Seaquist, Observation of resolved glucose signals in 1H NMR spectra of the human brain at 4 Tesla, Magn. Reson. Med. 36 (1996) 1–6.
[42] C. Cudalbu, A. Rengle, O. Beuf, S. Cavassila, Rat brain metabolite relaxation time estimates using magnetic resonance spectroscopy at two different field strengths, C.R. Chim. 11 (2008) 442–447.
[43] R. de Graaf, P. Brown, S. McIntyre, T. Nixon, K. Behar, D. Rothman, High magnetic field water and metabolite proton T_1 and T_2 relaxation in rat brain in vivo, Magn. Reson. Med. 56 (2006) 386–394.
[44] S. Michaeli, H. Gröhn, O. Gröhn, D.J. Sorce, C.S. Springer Jr., K. Ugurbil, M. Garwood, Exchange-influenced T_2 rho contrast in human brain images measured with adiabatic radio frequency pulses, Magn. Reson. Med. 53 (2005) 823–829.
[45] L. Xin, G. Gambarota, V. Mlynarik, R. Gruetter, Proton T_2 relaxation time of J-coupled cerebral metabolites in rat brain at 9.4 T, NMR Biomed. 21 (2008) 396–401.
[46] H. Lei, Y. Zhang, X.H. Zhu, W. Chen, Changes in the proton T_2 relaxation times of cerebral water and metabolites during forebrain ischemia in rat at 9.4 T, Magn. Reson. Med. 49 (2003) 979–984.
[47] M. Mescher, H. Merkle, J. Kirsch, M. Garwood, R. Gruetter, Simultaneous in vivo spectral editing and water suppression, NMR Biomed. 11 (1998) 266–272.
[48] T.W. Scheenen, A. Heerschap, D.W. Klomp, Towards 1H-MRSI of the human brain at 7 T with slice-selective adiabatic refocusing pulses, Magma 21 (2008) 95–101.
[49] I. Tkac, P.G. Henry, P. Andersen, C.D. Keene, W.C. Low, R. Gruetter, Highly resolved in vivo 1H NMR spectroscopy of the mouse brain at 9.4 T, Magn. Reson. Med. 52 (2004) 478–484.
[50] V.L. Yarnykh, Actual flip-angle imaging in the pulsed steady state: a method for rapid three-dimensional mapping of the transmitted radiofrequency field, Magn. Reson. Med. 57 (2007) 192–200.